HHS Public Access

Author manuscript

Clin Neurophysiol. Author manuscript; available in PMC 2022 December 01.

Published in final edited form as:

Clin Neurophysiol. 2021 December ; 132(12): 3197–3206. doi:10.1016/j.clinph.2021.07.028.

Individual localization value of resting-state fMRI in epilepsy presurgical evaluation: a combined study with stereo-EEG

Yingying Tang, MD[1,2], **Joon Yul Choi, PhD**[2], **Andreas Alexopoulos, MD**[2], **Hiroatsu Murakami, MD, PhD**[2], **Masako Daifu-Kobayashi, MD**[2], **Qin Zhou, MD**[2], **Imad Najm, MD**[2], **Stephen E Jones, MD, PhD**[3], **Zhong Irene Wang, PhD**[2,*]

[1]Department of Neurology, West China Hospital of Sichuan University, Chengdu, Sichuan, China

[2]Epilepsy Center, Cleveland Clinic, Cleveland, OH, USA

[3]Imaging Institute, Cleveland Clinic, Cleveland, OH, USA

Abstract

Objective: To examine the individual-patient-level localization value of resting-state functional MRI (rsfMRI) metrics for the seizure onset zone (SOZ) defined by stereo-electroencephalography (SEEG) in patients with medically intractable focal epilepsies.

Methods: We retrospectively included 19 patients who underwent SEEG implantation for epilepsy presurgical evaluation. Voxel-wise whole-brain analysis was performed on 3.0T rsfMRI to generate clusters for amplitude of low-frequency fluctuations (ALFF), regional homogeneity (ReHo) and degree centrality (DC), which were co-registered with the SEEG-defined SOZ to evaluate their spatial overlap. Subgroup and correlation analyses were conducted for different clinical characteristics.

Results: ALFF demonstrated concordant clusters with SEEG-defined SOZ in 73.7% of patients, with 93.3% sensitivity and 77.8% PPV. The concordance rate showed no significant difference when subgrouped by lesional/non-lesional MRI, SOZ location, interictal epileptiform discharges on scalp EEG, pathology or seizure outcomes. No significant correlation was seen between ALFF concordance rate and epilepsy duration, seizure-onset age, seizure frequency or number of antiseizure medications. ReHo and DC did not achieve favorable concordance results (10.5% and 15.8%, respectively). All concordant clusters showed regional activation, representing increased neural activities.

Conclusion: ALFF had high concordance rate with SEEG-defined SOZ at individual-patient level.

[*]**Corresponding author:** Zhong Irene Wang, Cleveland Clinic, Epilepsy Center, Desk S-51, 9500 Euclid Avenue, Cleveland, OH 44195, USA, Tel.: +1 216 444 8867, wangi2@ccf.org.

Conflict of Interest

All authors have no conflict of interest to disclose.

Significance: ALFF activation on rsfMRI can add localizing information for the noninvasive presurgical workup of intractable focal epilepsies.

Keywords

resting-state functional magnetic resonance imaging (rsfMRI); Stereo-electroencephalography (SEEG); epilepsy; presurgical evaluation; amplitude of low-frequency fluctuations (ALFF)

1. Introduction

Surgery is a major therapeutic option for patients with intractable focal epilepsies(Engel, 2018). To achieve the most favorable postoperative seizure outcomes, stereo-electroencephalography (SEEG) with three-dimensional (3D) brain sampling and high temporal/spatial resolution is often necessary in cases with difficult-to-localize epilepsies (Bulacio et al., 2012; Yan et al., 2019). Given the invasive nature and the inherent limitation of sampling extent(Yan et al., 2019), successful SEEG placement must rely on an optimal preimplantation hypothesis based on noninvasive evaluation data.

Noninvasive multimodal techniques, including structural magnetic resonance imaging (MRI), positron emission tomography (PET), magnetoencephalography (MEG), and ictal single-photon emission computerized tomography (SPECT), have been shown to play important roles in the planning of SEEG implantation and resective/ablative strategies(Murakami et al., 2016; Rossi Sebastiano et al., 2020; Wang et al., 2020, 2015). Resting-state functional MRI (rsfMRI), which aims at reflecting correlated activities across different brain regions by analyzing spontaneous fluctuation of blood-oxygen-level-dependent (BOLD) signal, has been widely used for mapping the epileptic network for different epilepsy syndromes and populations(Lang et al., 2014; Tracy and Doucet, 2015). Earlier group analysis showed that the BOLD signal was maximally abnormal in the ipsilateral mesial temporal area in patients with mesial temporal lobe epilepsy (TLE)(Zhang et al., 2010), and involvement of the ipsilateral hippocampus on the rsfMRI might serve as a marker to separate TLE with mesial temporal sclerosis (MTS) from TLE without MTS(Reyes et al., 2016). At individual patient level, potential localization value has also been corroborated by overlapping different rsfMRI measurements with the seizure onset zone (SOZ) delineated by subdural grid (SDG) implantation, not only in TLE(Stufflebeam et al., 2011; Weaver et al., 2013) but also in neocortical epilepsy(Jackson et al., 2017; Lee et al., 2014) and other epilepsy syndromes(Boerwinkle et al., 2018, 2017) for preoperative planning. Nonetheless, SDG implantation is inherently limited in its ability to sample from the 3D epileptic network and deep cortices(Bulacio et al., 2012; Yan et al., 2019). RsfMRI investigations combined with SEEG evaluation at the individual level could yield some new insight, but are currently lacking in the literature.

Analytic approaches on the rsfMRI signals are proposed to map the epileptic network broadly in 2 aspects - regional neural activities in different brain areas and functional integration among these areas(Lang et al., 2014; Tracy and Doucet, 2015), of which the former is more applicable for localization of the SOZ. Amplitude of low frequency fluctuation (ALFF), regional homogeneity (ReHo), and degree centrality (DC) are three

commonly used rsfMRI metrics to examine the regional neural activities, due to their ability to provide voxel-wise whole-brain information without any prior hypothesis(Chen et al., 2017; Jackson et al., 2017; Lang et al., 2014; Reyes et al., 2016; Tracy and Doucet, 2015; Weaver et al., 2013; Zhang et al., 2010). However, abnormalities detected by these three metrics often do not show complete concordance in their cerebral distribution(An et al., 2013; Ma et al., 2020), and could demonstrate different results for the same clinical populations(Fan et al., 2019; Lv et al., 2019). Therefore, when applying them on individual assessment for epilepsy, the question arises as to which one of these metrics has more efficacy to provide localization value.

To address these issues, we sought to comprehensively assess the agreement between the rsfMRI clusters measured by ALFF, ReHo as well as DC, and the SOZ defined by SEEG in patients with medically intractable focal epilepsies. Given that postoperative seizure freedom with complete SOZ resection is considered the best validation criteria for SOZ localization, we further did subgroup analysis based on postoperative seizure outcomes. Other subgroup and correlation analyses were also conducted for various clinical characteristics including seizure-onset age, epilepsy duration, seizure frequency, number of antiseizure medications (ASMs), MRI abnormality, SOZ location, scalp interictal epileptiform discharges (IEDs) and pathological findings. These analyses might clarify whether rsfMRI could serve as a useful additional noninvasive presurgical evaluation tool at individual level, and which rsfMRI metrics could offer possible candidate regions for SEEG implantation.

2. Materials and Methods

2.1 Study design

This retrospective, single-center study was approved by the Cleveland Clinic institutional review board (IRB). All subjects provided written informed consent prior to study participation. For each patient enrolled, decision about SEEG implantation was made at a clinical patient management conference (PMC) based on available multimodal data, including detailed history, neurological examination, semiology, video electroencephalography (EEG), MRI, PET, subtraction ictal SPECT co-registered with MRI (SISCOM) and MEG. Subsequent interpretation of SEEG findings and planning of surgery strategy were also discussed during PMC. The results of rsfMRI analyses were not used to inform any diagnostic and treatment recommendations. Our study workflow is detailed in Figure 1.

2.2 Participants

We reviewed a consecutive series of medically intractable focal epilepsy patients who were evaluated for surgery at Cleveland Clinic Epilepsy Center from 2017 to 2020. Patients who underwent both 3.0T rsfMRI and anatomical MRI scan with subsequent SEEG implantation were included. The exclusion criteria were: 1) age < 14 years or > 65 years; 2) head motion exceeding 3 mm in translation or 3 degrees in rotation during the rsfMRI scan. Thirty-nine healthy control subjects (HCs) were recruited, fulfilling the following inclusion criteria: 1) no neurological or psychiatric disorders; 2) no history of alcohol or other substance abuse; 3) no visible abnormalities on the anatomical MRI.

2.3 MRI data acquisition

MRI data were obtained using a Siemens 3.0 T scanner (Siemens Magnetom Prisma, USA) with a 32-channel phased array head coil. RsfMRI images were acquired using gradient echo echo-planar imaging (EPI) sequences: 39 axial slices, 180 volumes, TR = 2,170 ms, TE = 30 ms, thickness = 3 mm without gap, voxel size = 3×3×3 mm^3, FOV = 24 cm×24 cm, flip angle = 80°. T1-weighted images were acquired using a 3D MPRAGE sequence: 192 axial slices, thickness = 0.94 mm without gap, voxel size = 0.8×0.8×1 mm^3, TR = 1900 ms, TE = 2.57 ms, FOV = 24 cm×24 cm, flip angle = 10°.

2.4 MRI data processing

RsfMRI data was preprocessed using DPABI software package (https://rfMRI.org/dpabi) in MATLAB 2015a (MathWorks, Natick, MA, USA) with the following steps(Yan et al., 2016): 1) removing the first 10 time points to allow signal equilibrium and subjects' adaptation; 2) slice timing and rigid-body realignment; 3) removing linear trend of the time course; 4) regressing out covariates from head motion, cerebrospinal fluid signal and white matter signal; 5) spatial normalization to the Montreal Neurological Institute (MNI) space with a resampling voxel size of 3×3×3 mm^3; 6) band-pass filtering (0.01–0.08Hz). Then, ALFF, ReHo and DC were calculated for each voxel of the entire brain, and spatial smoothing with an isotropic Gaussian kernel with a full width at half maximum (FWHM) of 4 mm was applied(Yu-Feng et al., 2007; Zang et al., 2004; Zuo et al., 2012). Lastly, the rsfMRI clusters were converted back to the native individual space by applying the transformation information derived from the spatial normalization process.

2.5 RsfMRI clusters generation

For all three rsfMRI metrics, differences between each individual patient and 39 HCs were identified using a two-sample t test by SPM12 in MATLAB R2015a (MathWorks, Natick, Massachusetts; https://www.fil.ion.ucl.ac.uk/spm/software/spm12/), with a significance threshold of $P<0.001$ with false discovery rate (FDR) correction. Given that subcortical nucleus and white matter are not considered to be the primary target for SEEG implantation and surgery in patients with focal epilepsies, we limited the results with a binarized cortical mask generated based on AAL template(Tzourio-Mazoyer et al., 2002) in SPM12. In cases with scattered rsfMRI clusters in multiple brain regions, the clusters with the top-3 peak intensity (indicated by t-value) were empirically taken into account as candidates for the concordance analysis.

2.6 Concordance between rsfMRI clusters and SEEG-defined SOZ

Co-registration was performed in the Curry 8 software (Compumedics Neuroscan, Charlotte, NC, USA) for each patient. SEEG electrode locations were identified by fusing the post-implantation high-resolution CT with the pre-implantation MRI (details in Figure 1). The SOZ was delineated by the ictal contacts based on the official clinical report of SEEG, which was finalized according to PMC consensus. After coregistration, the pre-implantation MRI, rsfMRI clusters, SEEG electrode locations, and postoperative MRI could be displayed and evaluated in the same space. Concordance was determined by rsfMRI clusters spatially overlapping with the SOZ at the same sublobar location(Lee et al., 2014); while discordance

was determined by no overlap. If no rsfMRI cluster could survive after FDR correction, the result was considered negative.

2.7 Definition of clinical characteristics

For statistical testing, we categorized seizure frequency as daily, weekly and monthly. Brain MRI finding was classified as lesional and non-lesional according to the official radiology report by visual inspection on the clinical epilepsy-protocol 3.0T MRI. The SOZs located in the basal and/or mesial aspect of the brain (such as orbitofrontal, mesial temporal, insula, mesial frontal, and mesial parietal) were grouped as deep-seated areas, relative to the group of SOZs in the convexity of brain. Interictal scalp EEG data with the same ASM regimen and the closest date to the rsfMRI scan were reviewed and categorized as subgroups with IEDs or those without. The localization of the IEDs were retrieved from the official medical report. Pathological classification of surgical specimens was based on the International League Against Epilepsy (ILAE) recommendation of neuropathology workup(Blümcke et al., 2016) and focal cortical dysplasia (FCD) classification guidelines(Blümcke et al., 2011). For patients with postoperative follow-up more than 1 year, surgical outcomes were defined using ILAE classifications(Wieser et al., 2008) and further dichotomized as seizure-free (ILAE class 1) or non-seizure-free (ILAE class 2–6). The last surgery date was selected as the start of follow-up when the patient underwent multiple surgeries.

2.8 Statistical analysis

Concordance rate was evaluated separately for ALFF, ReHo and DC clusters, as well as the estimated sensitivity and positive predicted values (PPV) with corresponding 95% confidence intervals (CIs). Pearson $\chi 2$ test or Fisher exact test for proportions, when appropriate, was used to compare concordance rates in subgroups of patients with various clinical factors including anatomic MRI abnormality, SOZ location, scalp IEDs, seizure outcome and pathological findings. Spearman correlation coefficient was used to assess the relationship between concordance rate and epilepsy duration, seizure onset age, seizure frequency and number of ASMs. Student's t test for continuous data with normal distribution and Pearson $\chi 2$ test for categorical data was conducted to compare the demographic data between the patients and the HCs. All statistical analysis was performed in SPSS 20.0 (http://www.spss.com/) at a significant level of 0.05, two-sided.

3. Results

3.1 Cohort overview

A total of 19 patients were included in this study (mean ± standard deviation (SD) age: 29.4±14.7 years, 12 male/ 7 female, 16 right-handed/ 2 left-handed), which was not significantly different from the HCs (mean ± SD age: 25.9±4.5 years, 17 male/ 22 female, 33 right-handed/ 6 left-handed, detailed in Supplementary Table S1. The average seizure onset age was 13.7 years (range=1 to 48) with an average epilepsy duration of 15.6 years (range=4 to 51). Sixteen patients underwent further surgery (10 with resection, 5 with laser ablation, 1 with laser followed by resection). Patient demographics and clinical characteristics are provided in Table 1.

3.2 Concordance evaluation

As summarized in Table 2 and Supplementary Table S2, ALFF showed concordant clusters with the SEEG-defined SOZ in 14/19 patients (73.7%, 95% CI, 48.8% - 90.9%), with the sensitivity of 93.3% (95% CI, 66.0% - 99.7%) and PPV of 77.8% (95% CI, 51.9% - 92.6%). ReHo and DC only exhibited concordant clusters in 2/19 (10.5%) and 3/19 (15.8%) patients, respectively. The majority of the patients reported negative results in ReHo (N=11/19, 57.9%) and DC (N=12/19, 63.2%), i.e. no cluster survived after correction. When using more lenient thresholds (P_{FDR}< 0.005, 0.01 and 0.05) for ReHo and DC, the yields of concordant clusters did not change significantly. Among all the cases with concordant rsfMRI clusters, ALFF, ReHo and DC showed regional activation (examples shown in Figure 2 and Figure 3), indicating significantly increased spontaneous neural activities compared to HCs. Figure 2 shows a representative case with a dysplastic MRI lesion of unclear boundary at the left basomedial temporo-occipital area (P1 in Table 1). ALFF generated an activation cluster in the left fusiform gyrus, which was located within the SOZ defined by SEEG and smaller in size than the MRI lesion. SEEG-guided left temporal lobectomy was performed with histopathological confirmation of FCD type I. This patient was seizure-free for 1.75 years at the most recent follow-up. Figure 3 shows another representative case with non-lesional MRI (P7 in Table 1). ALFF generated two activation clusters, both concordant with the SEEG-defined SOZ in the left dorsomedial parietal lobe along the marginal sulcus. SEEG-guided left mesial parietal corticectomy was performed with histopathological confirmation of FCD type IIA. Postoperative MRI showed that the SEEG-defined SOZ as well as the ALFF clusters were not completely included in the resection. This patient did not achieve seizure freedom and additional surgery has been recommended at PMC to extend the resection.

3.3 Subgroup and correlation analysis

Subgroup and correlation analysis were carried out only for ALFF, due to the low yield of ReHo and DC. ALFF showed no difference in concordance rate between the lesional MRI (80.0%, 8/10) and the non-lesional MRI subgroups (66.7%, 6/9, χ^2= 1.29, p= 0.78), or the TLE (77.8%, 7/9) and the extratemporal lobe epilepsy (ETLE) subgroups (70.0%, 7/10, χ^2= 1.83, p= 0.58). Although the patients with deep-seated SOZs had a higher ALFF concordance rate (13/16; 81.3%) than the patients with SOZs located at the convexity of brain (1/3; 33.3%), it was not statistically significant (χ^2=4.98, p=0.07). The concordance rate of ALFF also seemed higher in patients with IEDs on scalp EEG (10/12, 83.3%) than those without (4/7, 57.1%), but this finding also did not reach statistical significance (χ^2=2.41, P=0.36). Details are listed in Table 3. No correlation was detected between the ALFF concordance rate and the clinical parameters (age, epilepsy duration, seizure onset age, seizure frequency and number of ASMs, P>0.05, details in Supplementary Table S3).

In the 11 patients who underwent resection, histopathological examination revealed 5 FCD type I, 2 FCD type IIA, 1 FCD type IIB, 1 heterotopia, and 2 double pathology (heterotopia plus FCD type IB). The 2 patients with double pathology exhibited concordant ALFF cluster in the region of FCD, not in the nodules. Although no statistical difference was observed in ALFF concordance rate when subgrouped by pathological categories (χ^2= 8.99, p = 0.36, Table 3), the ALFF performed well in generating concordant clusters in FCD (8/10, 80%).

Postoperative seizure outcomes were assessed in 8 patients with more than 1 year follow-up (range=1.5 to 2.5 years; mean: 2.2 years). Six patients became seizure-free (ILAE class 1); 2 patients did not become seizure-free (1 with ILAE class 4 and the other with ILAE class 5). There was no difference in ALFF concordance rate between the seizure-free and the non-seizure-free subgroups (χ^2= 1.21, p = 1.00, Table 3). For the 2 patients who had ALFF clusters concordant with SEEG-defined SOZ but did not become seizure-free, the SOZ as well as the ALFF clusters were not completely included in the resection, and a second surgery was proposed (example in Figure 3).

4. Discussion

Our study is the first to comprehensively assess individual-level localization value of the noninvasive metrics of rsfMRI in terms of their concordance with the SEEG-defined SOZ. With no bias from *a priori* hypothesis, ALFF, ReHo and DC were selected to generate candidate foci via voxel-wise whole-brain analysis in a consecutive cohort of medically intractable focal epilepsy patients who underwent presurgical evaluation. Among these 3 metrics, ALFF yielded a high concordance rate with the SOZ defined by SEEG. This finding suggests that rsfMRI, specifically the ALFF metric, might be able to add supplementary information for epilepsy presurgical evaluation on an individual level.

RsfMRI Metrics

ALFF, ReHo and DC are 3 classical metrics for characterizing the local properties of the rsfMRI signal from different perspectives, which are reported to have different performances and are complimentary to each other(Lang et al., 2014; Tracy and Doucet, 2015; Yu-Feng et al., 2007; Zang et al., 2004; Zuo et al., 2012). In patients with migraine, all 3 metrics showed well-overlapped decrease within the sensorimotor area (Zhang et al., 2017). On the contrary, mismatched clusters among these 3 metrics were observed in patients with attention-deficit/hyperactivity disorder(An et al., 2013) and facial synkinesis(Ma et al., 2020). Drastically different distribution among these 3 metrics was found in patients with transient ischemic attack(Lv et al., 2019) and brain tumors(Fan et al., 2019). Our study also showed different performances among the 3 metrics; SOZ co-localization was shown in 74% of patients by ALFF, but only 16% by DC and 11% by ReHo. Although more future studies are needed to further clarify the differing roles of these 3 metrics in the epileptic brain, it is generally considered that ALFF measures the intensity of BOLD fluctuations at each voxel(Yu-Feng et al., 2007), thereby our results suggest regional higher-intensity BOLD fluctuations might mark the SOZ. ReHo measures the time course coherence of a given voxel with its nearest neighbors(Zang et al., 2004), and DC measures the connection numbers of a given voxel to the entire brain(Zuo et al., 2012); these two measures more likely reflect the interaction of the SOZ with other brain region, short or long distance, within the epileptic network.

Our results highlight the value of ALFF in SOZ localization with a high sensitivity and PPV. Such potential localization value of ALFF is consistent with prior group-level studies in patients with TLE(Reyes et al., 2016; Zhang et al., 2010). A recent study reported that ALFF identified the putative epileptogenic zone in 45% patients with focal epilepsy at individual level(Chen et al., 2017). The relatively lower yield of their study as compared to ours might

be due to methodological differences, and the patient cohort and control groups selected. In line with previous studies(Chen et al., 2017; Zhang et al., 2010), we detected *activation* in the SOZ-concordant ALFF clusters, rather than *deactivation*. This indicates an increase of regional neural activities, which has also been supported by other rsfMRI measurements using different analytic approaches(Chen et al., 2017; Jackson et al., 2017; Stufflebeam et al., 2011; Yan et al., 2020). Although the neurophysiology for ALFF increase inside the SOZ is still unclear, its association with the interictal epileptic activity has been suggested by a prior study(Zhang et al., 2010). Given that the interictal epileptic activities can reflect the primary irritative component of the epileptogenic zone(Bonini et al., 2014; Malinowska et al., 2014), it is reasonable that ALFF activations co-localized with SEEG-defined SOZ in our study.

ReHo and DC did not deliver high yields for SOZ localization, as shown by our data. Jackson et al. reported an epilepsy case with bottom-of-sulcus dysplasia in the language cortex, with a ReHo activation focus showing much smaller extent than the PET and SPECT abnormalities, which helped formulate a successful, tailored corticectomy procedure(Jackson et al., 2017). DC, as a relatively new metric, has not yet been attempted by prior studies to localize SOZ. In addition to ALFF, ReHo and DC, other rsfMRI metrics have also been reported to assist epilepsy localization. For example, rsfMRI foci generated by intrinsic connectivity contrast (ICC) has been reported to overlap with 72% of the SOZs identified by SDG in 29 patients with epilepsy surgery(Lee et al., 2014). A prospective study in a heterogeneous pediatric intractable epilepsy population used independent component analysis (ICA) to achieve up to 90% agreement between the rsfMRI foci and the SDG-detected SOZs(Boerwinkle et al., 2017). In another study from the same group, ICA-determined SOZ was used to guide epilepsy surgery prospectively in a pediatric cohort, demonstrating improved seizure-freedom(Boerwinkle et al., 2019). A recent meta-analysis also demonstrated the potential value of rsfMRI with ICA in SOZ localization versus traditional methods(Chakraborty et al., 2020), pointing towards the direction of utilizing information from rsfMRI to contribute to noninvasive presurgical planning.

RsfMRI and Intracranial EEG

All prior studies examined rsfMRI metrics together with SDG recording and/or surgery field. Our current study is the first attempt for a combined study of rsfMRI metrics and SEEG. The concordance rate as well as sensitivity and PPV in our data were similar to those achieved with PET, MEG, SPECT and structural MRI post-processing when compared to SEEG localization(Murakami et al., 2016; Rossi Sebastiano et al., 2020; Wang et al., 2020, 2015). Although no single test can measure all properties of the entire epileptic network, integrating multimodal information typically benefits hypothesis generation for SEEG and further resective/ablative strategies. With no requirement of *a priori* hypothesis, rsfMRI could be added to the test battery of established noninvasive methods to provide complimentary information for SEEG preimplantation planning.

In addition to seizure localization, combined signal analysis on rsfMRI and intracranial EEG data has made significant recent advances on understanding brain networks in general. Prior studies demonstrated high similarities between the rsfMRI-based networks and the

electrocorticography (ECoG)-based networks at the individual level(Kucyi et al., 2018; Yan et al., 2020). Different network patterns could be found for different frequency bands(Kucyi et al., 2018), and the carrier frequency ranging from alpha to low-beta (8–32Hz) was shown to correlate best with the rsfMRI network(Yan et al., 2020). Future studies that correlate rsfMRI metrics to distinct SEEG seizure-onset patterns in specific frequency bands, would likely facilitate our understanding of the electrophysiological basis of the rsfMRI metrics and characterization of the epileptic networks.

Subgroup Analyses

We performed subgroup analyses in this pilot study, recognizing the small sample size would influence subgroup findings. Although none of the findings reached statistical significance, some trends were notable, and warrant future larger studies for confirmation and validation.

Our data showed a trend that ALFF appeared to have a higher concordance rate in the patients with deep-seated SOZ than the patients with SOZs located at the convexity of brain (81.3% vs. 33.3%, p=0.07). Lee et al. observed the same tendency in patients with TLE that the rsfMRI foci demonstrated higher concordance in mesial SOZ than lateral SOZ using ICC-map(Lee et al., 2014). They also reported that concordance was higher in patients with ETLE compared to TLE, which was not seen in our study.

The performance of ALFF did not differ in our study between subgroups with lesional MRI and non-lesion MRI. A prior study on heterogeneous brain tumors illustrated that ALFF alterations were not equivalent to structural lesion extent(Fan et al., 2019). In line with this previous study, the detected ALFF clusters in our study had markedly smaller size than the lesions (Figure 3), or could even be distributed in different areas of the lesions (P11 and P18 in Table 1), which supports the notion that rsfMRI provides supplementary information for brain regional neural activities, rather than the structural extent of lesion.

Another trend noted in our study is that patients with IEDs on the scalp EEG seemed more likely to have SOZ-concordant ALFF activation clusters, compared to those without IEDs (83.3% vs. 57.1%, P=0.36). It is consistent with a previous simultaneous EEG-fMRI study, showing significant correlation between the increased ALFF and the IED numbers(Zhang et al., 2010). This might suggest that the patients with IEDs on the scalp EEG could more likely benefit from rsfMRI to obtain localizable ALFF clusters.

Limitations

Several limitations should be noted:

1. Our study was limited by its relatively small sample size, which may reduce the power to detect some potential differences when conducting subgroup comparisons. The same limitation applies to the HC group in this study. To ensure the rsfMRI data of the individual patient to be more comparable to that of the HCs, we only used data from our single center with a strictly identical scan protocol, rather than pulling rsfMRI data from multi-site data repositories, which was commonly used for between-group analysis.

2. Patients who need SEEG implantation with difficult-to-localize SOZ were included in this study; therefore, there is an inevitable selection bias and the cohort could not represent the general population of epilepsy patients undergoing presurgical evaluation.

3. There was a relative lack of heterogeneity in pathology, in that FCD constituted the major etiology in our cohort. This pathology composition is comparable with other SEEG investigations(Grinenko et al., 2018; Murakami et al., 2016; Wang et al., 2020), suggesting the challenging nature of evaluating patients with FCD, especially when the MRI is non-lesional. Also, laser ablation prevented detailed review of surgical pathology in 5 patients.

4. In cases with scattered rsfMRI clusters in multiple brain regions, we empirically took the clusters with top-3 peak intensity into account in the concordance analysis. Further study which examines different thresholds may improve the performance of rsfMRI in SOZ localization by estimating an optimal cut-off.

5. Further extension of the postoperative follow-up period is needed to evaluate the localization value of rsfMRI in terms of long-term prognosis. Overall, significant future work needs to be performed to improve the PPV and sensitivity of the current methods, for maximizing their values to be added to the clinical protocol for pre-surgical workup.

5. Conclusions

We provide the first study to examine the localization value of rsfMRI metrics for SOZ defined by SEEG at the individual level. ALFF demonstrated concordant clusters with SEEG-defined SOZ in 73.7% of patients. All concordant clusters showed regional activation, representing increased neural activities. Neither ReHo nor DC localized the SEEG-defined SOZ well, supporting that the three rsfMRI metrics represent regional neural activities from different perspectives. Our findings suggest that ALFF activation may add supplementary, noninvasive information for epilepsy presurgical evaluation, contributing to SEEG implantation and further surgical strategy planning for individuals with medically intractable focal epilepsy.

Supplementary Material

Refer to Web version on PubMed Central for supplementary material.

Acknowledgements

We thank all the patients and healthy controls who participated in this study.

Funding

This work was supported by National Institutes of Health [grant number R01 NS109439].

Abbreviations:

ALFF	Amplitude of low frequency fluctuation

ASMs	antiseizure medications
BOLD	blood-oxygen-level-dependent
CIs	confidence intervals
DC	degree centrality
ECoG	electrocorticography
EEG	electroencephalograph
ETLE	extratemporal lobe epilepsy
FCD	focal cortical dysplasia
FDR	false discovery rate
HCs	healthy control subjects
ICA	independent component analysis
ICC	intrinsic connectivity contrast
IEDs	interictal epileptiform discharges
ILAE	International League Against Epilepsy
MEG	magnetoencephalography
MNI	Montreal Neurological Institute
MRI	magnetic resonance imaging
MTS	mesial temporal sclerosis
PET	positron emission tomography
PMC	patient management conference
PPV	positive predicted values
ReHo	regional homogeneity
SDG	subdural grid
SEEG	Stereo-electroencephalography
SISCOM	subtraction ictal SPECT co-registered with MRI
SOZ	seizure onset zone
SPECT	single-photon emission computerized tomography
TLE	temporal lobe epilepsy
3D	three-dimensional

References

An L, Cao Q-J, Sui M-Q, Sun L, Zou Q-H, Zang Y-F, et al. Local synchronization and amplitude of the fluctuation of spontaneous brain activity in attention-deficit/hyperactivity disorder: a resting-state fMRI study. Neurosci Bull 2013;29:603–13. [PubMed: 23861089]

Blümcke I, Aronica E, Miyata H, Sarnat HB, Thom M, Roessler K, et al. International recommendation for a comprehensive neuropathologic workup of epilepsy surgery brain tissue: A consensus Task Force report from the ILAE Commission on Diagnostic Methods. Epilepsia 2016;57:348–58. [PubMed: 26839983]

Blümcke I, Thom M, Aronica E, Armstrong DD, Vinters H V., Palmini A, et al. The clinicopathologic spectrum of focal cortical dysplasias: A consensus classification proposed by an ad hoc Task Force of the ILAE Diagnostic Methods Commission1. Epilepsia 2011;52:158–74. [PubMed: 21219302]

Boerwinkle VL, Cediel EG, Mirea L, Williams K, Kerrigan JF, Lam S, et al. Network-targeted approach and postoperative resting-state functional magnetic resonance imaging are associated with seizure outcome. Ann Neurol 2019;86:344–56. [PubMed: 31294865]

Boerwinkle VL, Foldes ST, Torrisi SJ, Temkit H, Gaillard WD, Kerrigan JF, et al. Subcentimeter epilepsy surgery targets by resting state functional magnetic resonance imaging can improve outcomes in hypothalamic hamartoma. Epilepsia 2018;59:2284–95. [PubMed: 30374947]

Boerwinkle VL, Mohanty D, Foldes ST, Guffey D, Minard CG, Vedantam A, et al. Correlating Resting-State Functional Magnetic Resonance Imaging Connectivity by Independent Component Analysis-Based Epileptogenic Zones with Intracranial Electroencephalogram Localized Seizure Onset Zones and Surgical Outcomes in Prospective Pediatric In. Brain Connect 2017;7:424–42. [PubMed: 28782373]

Bonini F, McGonigal A, Trébuchon A, Gavaret M, Bartolomei F, Giusiano B, et al. Frontal lobe seizures: From clinical semiology to localization. Epilepsia 2014;55:264–77. [PubMed: 24372328]

Bulacio JC, Jehi L, Wong C, Gonzalez-Martinez J, Kotagal P, Nair D, et al. Long-term seizure outcome after resective surgery in patients evaluated with intracranial electrodes. Epilepsia 2012;53:1722–30. [PubMed: 22905787]

Chakraborty AR, Almeida NC, Prather KY, O'Neal CM, Wells AA, Chen S, et al. Resting-state functional magnetic resonance imaging with independent component analysis for presurgical seizure onset zone localization: A systematic review and meta-analysis. Epilepsia 2020;61:1958–68. [PubMed: 32770853]

Chen Z, An Y, Zhao B, Yang W, Yu Q, Cai L, et al. The value of resting-state functional magnetic resonance imaging for detecting epileptogenic zones in patients with focal epilepsy. PLoS One 2017;12:e0172094. [PubMed: 28199371]

Engel J The current place of epilepsy surgery. Curr Opin Neurol 2018;31:192–7. [PubMed: 29278548]

Fan Z, Chen X, Qi Z-X, Li L, Lu B, Jiang C-L, et al. Physiological significance of R-fMRI indices: Can functional metrics differentiate structural lesions (brain tumors)? NeuroImage Clin 2019;22:101741. [PubMed: 30878611]

Grinenko O, Li J, Mosher JC, Wang IZ, Bulacio JC, Gonzalez-Martinez J, et al. A fingerprint of the epileptogenic zone in human epilepsies. Brain 2018;141:117–31. [PubMed: 29253102]

Jackson GD, Pedersen M, Harvey AS. How small can the epileptogenic region be? Neurology 2017;88:2017–9. [PubMed: 28446651]

Kucyi A, Schrouff J, Bickel S, Foster BL, Shine JM, Parvizi J. Intracranial electrophysiology reveals reproducible intrinsic functional connectivity within human brain networks. J Neurosci 2018;38:4230–42. [PubMed: 29626167]

Lang S, Duncan N, Northoff G. Resting-State Functional Magnetic Resonance Imaging. Neurosurgery 2014;74:453–65. [PubMed: 24492661]

Lee HW, Arora J, Papademetris X, Tokoglu F, Negishi M, Scheinost D, et al. Altered functional connectivity in seizure onset zones revealed by fMRI intrinsic connectivity. Neurology 2014;83:2269–77. [PubMed: 25391304]

Lv Y, Li L, Song Y, Han Y, Zhou C, Zhou D, et al. The Local Brain Abnormalities in Patients With Transient Ischemic Attack: A Resting-State fMRI Study. Front Neurosci 2019;13:24y. [PubMed: 30804735]

Ma J, Hua X-Y, Zheng M-X, Wu J-J, Huo B-B, Xing X-X, et al. Spatial patterns of intrinsic brain activity and functional connectivity in facial synkinesis patients. Br J Neurosurg 2020 6 5;1–6. doi: 10.1080/02688697.2020.1773396.

Malinowska U, Badier J-M, Gavaret M, Bartolomei F, Chauvel P, Bénar C-G. Interictal networks in Magnetoencephalography. Hum Brain Mapp 2014;35:2789–805. [PubMed: 24105895]

Murakami H, Wang ZI, Marashly A, Krishnan B, Prayson RA, Kakisaka Y, et al. Correlating magnetoencephalography to stereo-electroencephalography in patients undergoing epilepsy surgery. Brain 2016;139:2935–47. [PubMed: 27567464]

Reyes A, Thesen T, Wang X, Hahn D, Yoo D, Kuzniecky R, et al. Resting-state functional MRI distinguishes temporal lobe epilepsy subtypes. Epilepsia 2016;57:1475–84. [PubMed: 27374869]

Rossi Sebastiano D, Tassi L, Duran D, Visani E, Gozzo F, Cardinale F, et al. Identifying the epileptogenic zone by four non-invasive imaging techniques versus stereo-EEG in MRI-negative pre-surgery epilepsy patients. Clin Neurophysiol 2020;131:1815–23. [PubMed: 32544836]

Stufflebeam SM, Liu H, Sepulcre J, Tanaka N, Buckner RL, Madsen JR. Localization of focal epileptic discharges using functional connectivity magnetic resonance imaging. J Neurosurg 2011;114:1693–7. [PubMed: 21351832]

Tracy JI, Doucet GE. Resting-state functional connectivity in epilepsy. Curr Opin Neurol 2015;28:158–65. [PubMed: 25734954]

Tzourio-Mazoyer N, Landeau B, Papathanassiou D, Crivello F, Etard O, Delcroix N, et al. Automated Anatomical Labeling of Activations in SPM Using a Macroscopic Anatomical Parcellation of the MNI MRI Single-Subject Brain. Neuroimage 2002;15:273–89. [PubMed: 11771995]

Shan Wang, Tang Y, Aung T, Chen C, Katagiri M, Jones SE, et al. Multimodal noninvasive evaluation in MRI-negative operculoinsular epilepsy. J Neurosurg 2020;132:1334–44.

Wang ZI, Jones SE, Jaisani Z, Najm IM, Prayson RA, Burgess RC, et al. Voxel-based morphometric magnetic resonance imaging (MRI) postprocessing in MRI-negative epilepsies. Ann Neurol 2015;77:1060–75. [PubMed: 25807928]

Weaver KE, Chaovalitwongse WA, Novotny EJ, Poliakov A, Grabowski TG, Ojemann JG. Local functional connectivity as a pre-surgical tool for seizure focus identification in non-lesion, focal epilepsy. Front Neurol 2013;4:43. [PubMed: 23641233]

Wieser HG, Blume WT, Fish D, Goldensohn E, Hufnagel A, King D, et al. Proposal for a New Classification of Outcome with Respect to Epileptic Seizures Following Epilepsy Surgery. Epilepsia 2008;42:282–6.

Yan C-G, Wang X-D, Zuo X-N, Zang Y-F. DPABI: Data Processing & Analysis for (Resting-State) Brain Imaging. Neuroinformatics 2016;14:339–51. [PubMed: 27075850]

Yan H, Katz JS, Anderson M, Mansouri A, Remick M, Ibrahim GM, et al. Method of invasive monitoring in epilepsy surgery and seizure freedom and morbidity: A systematic review. Epilepsia 2019;60:1960–72. [PubMed: 31423575]

Yan Y, Qian T, Xu X, Han H, Ling Z, Zhou W, et al. Human cortical networking by probabilistic and frequency-specific coupling. Neuroimage 2020;207:116363. [PubMed: 31740339]

Yu-Feng Z, Yong H, Chao-Zhe Z, Qing-Jiu C, Man-Qiu S, Meng L, et al. Altered baseline brain activity in children with ADHD revealed by resting-state functional MRI. Brain Dev 2007;29:83–91. [PubMed: 16919409]

Zang Y, Jiang T, Lu Y, He Y, Tian L. Regional homogeneity approach to fMRI data analysis. Neuroimage 2004;22:394–400. [PubMed: 15110032]

Zhang J, Su J, Wang M, Zhao Y, Zhang Q-T, Yao Q, et al. The sensorimotor network dysfunction in migraineurs without aura: a resting-state fMRI study. J Neurol 2017;264:654–63. [PubMed: 28154971]

Zhang Z, Lu G, Zhong Y, Tan Q, Chen H, Liao W, et al. fMRI study of mesial temporal lobe epilepsy using amplitude of low-frequency fluctuation analysis. Hum Brain Mapp 2010;31:1851–61. [PubMed: 20225278]

Zuo X-N, Ehmke R, Mennes M, Imperati D, Castellanos FX, Sporns O, et al. Network Centrality in the Human Functional Connectome. Cereb Cortex 2012;22:1862–75. [PubMed: 21968567]

Highlights

1. First study to examine the localization value of resting-state fMRI metrics for seizure onset zone (SOZ) defined by SEEG at the individual level.
2. Amplitude of low-frequency fluctuations (ALFF) demonstrated concordant clusters with SEEG-defined SOZ in 73.7% of patients.
3. All concordant clusters showed regional activation, representing increased neural activities.
4. Results suggest ALFF activation on resting-state fMRI can add localization information for SOZ for individuals with intractable focal epilepsies.

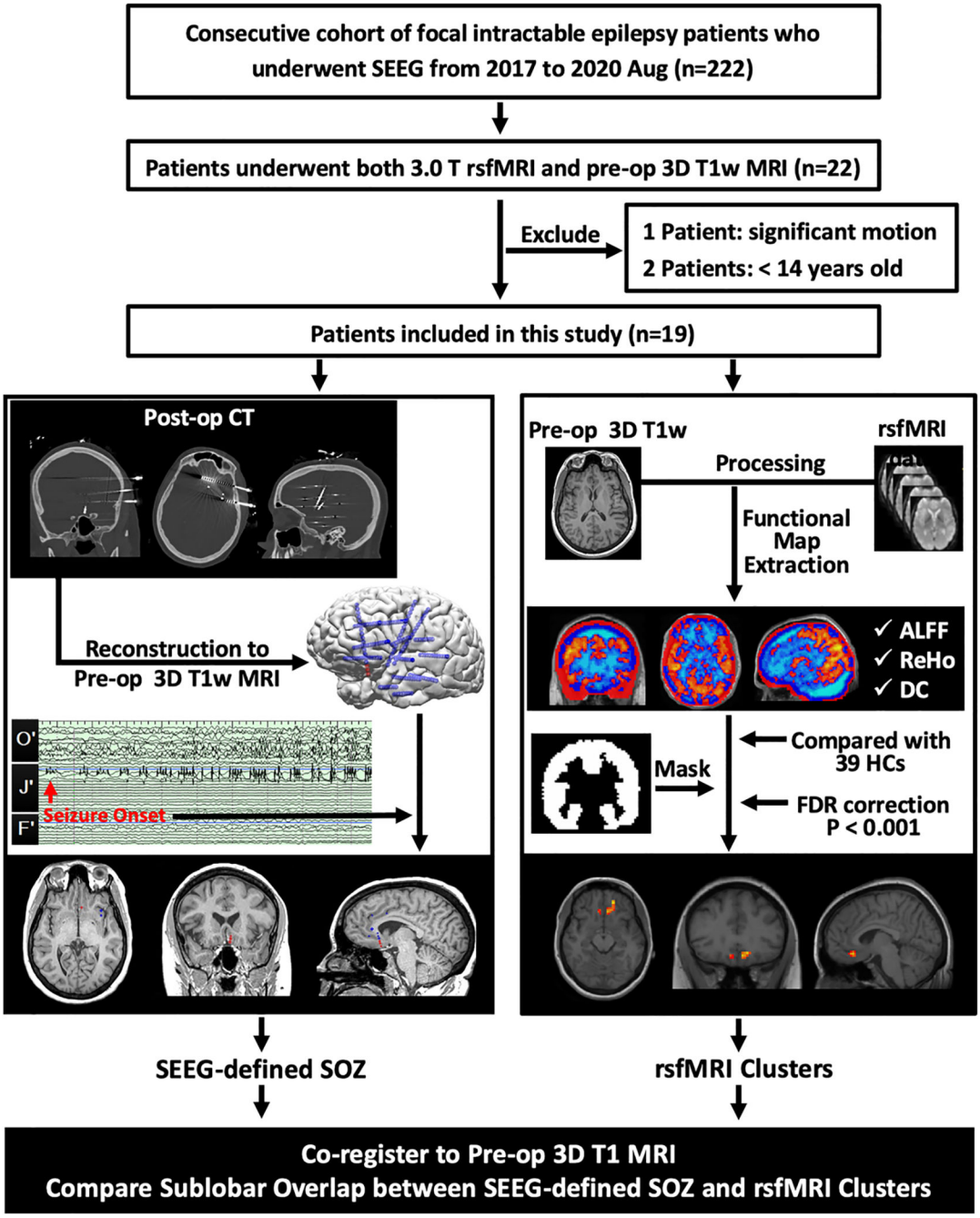

Figure 1:

Workflow of data collection, processing and analysis. Patients were included from a consecutive cohort of medically intractable focal epilepsy patients with SEEG implantation. SEEG-defined SOZ contacts were retrieved from the finalized clinical report after consensus discussion at the patient management conference. RsfMRI clusters were generated for each patient by comparison with 39 HCs. ALFF, ReHo and DC clusters underwent concordance assessment with the SEEG-defined SOZ.

SEEG= Stereo-electroencephalography; rsfmri= resting-state functional magnetic resonance imaging; Pre-op= preoperative; 3D= three dimensional; T1w= T1-weighted; Post-im= post-

implantation; CT= computed tomography; SOZ= seizure onset zone; ALFF= amplitude of low-frequency fluctuations; ReHo= regional homogeneity; DC= degree centrality; HCs= healthy control subjects; FDR= False Discovery Rate.

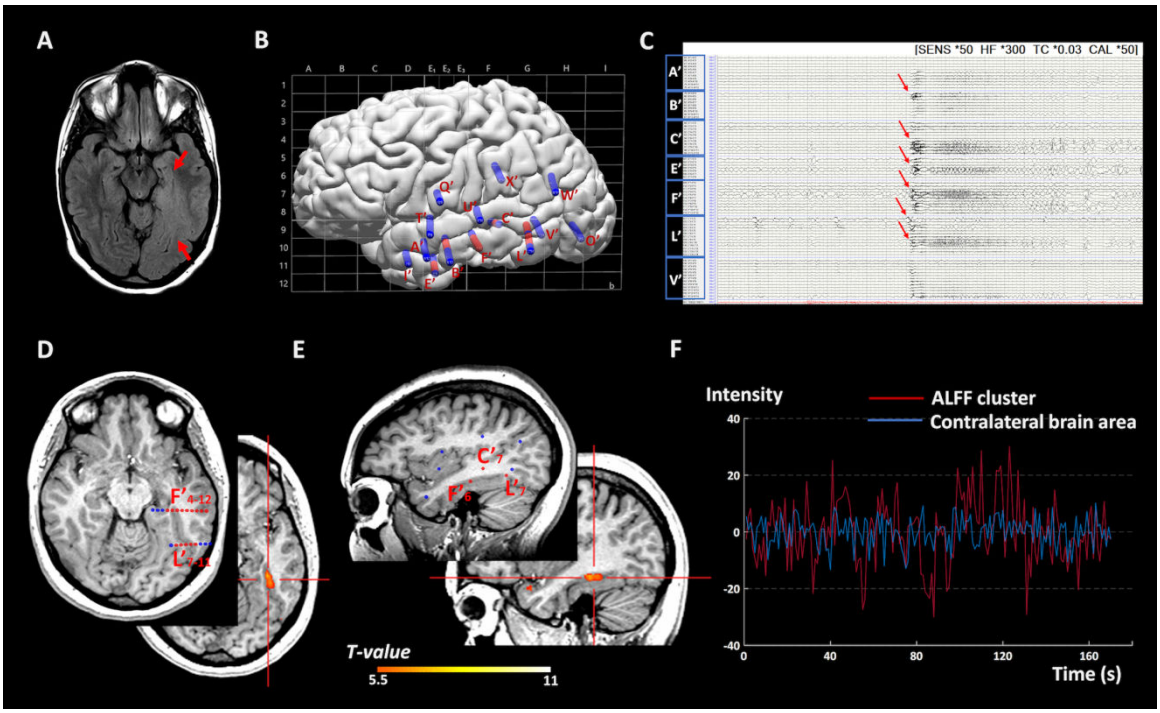

Figure 2:

Representative case 1: Illustration of a concordant ALFF cluster with the SEEG-defined SOZ in a patient with a widespread dysplastic MRI lesion of unclear boundary at the left basomedial temporo-occipital area (P1 in table 1). SEEG was performed to help delineate the extent of the SOZ, especially the involvement of the ipsilateral hippocampus anteriorly, speech area dorsally and visual area posteriorly. A) 3T 2D FLAIR image showing abnormal hyperintensity signal extending from the left hippocampus to the occipital lobe (red arrows). B) SEEG implantation map shown with Talairach grid superimposed, including 14 electrodes and 160 contacts (contacts indicating SOZ marked with red, other contacts marked with blue). C) Bipolar montage of relevant SEEG channels (20-second epoch): Typical seizure showed onset involving primarily contacts L'1–5 (lesion), L'7–11 and F'4–12 (basal temporal region) along with E'4–7, B'3–6 (anterior temporal region) and C'7–11 (superior temporal sulcus) characterized by paroxysmal low amplitude fast activity (red arrows). D) axial view and E) sagittal view: The ALFF activation cluster, indicated by the red crossbar, was located inside the SOZ noted by the red SEEG contacts. F) time series plots of the BOLD signal fluctuation versus time in seconds. Time series were extracted from the peak of the SOZ-concordant ALFF activation cluster in the left fusiform gyrus (red line) showed significantly higher amplitude than that of the corresponding contralateral brain area (blue line), which suggests increase of regional neural activities within the SOZ. This patient has been seizure-free for 1.75 years following left temporal lobectomy.

ALFF= amplitude of low-frequency fluctuations; s= second; SOZ= seizure onset zone; SEEG= Stereo-electroencephalography; MRI= magnetic resonance imaging; BOLD= Blood oxygenation level dependent.

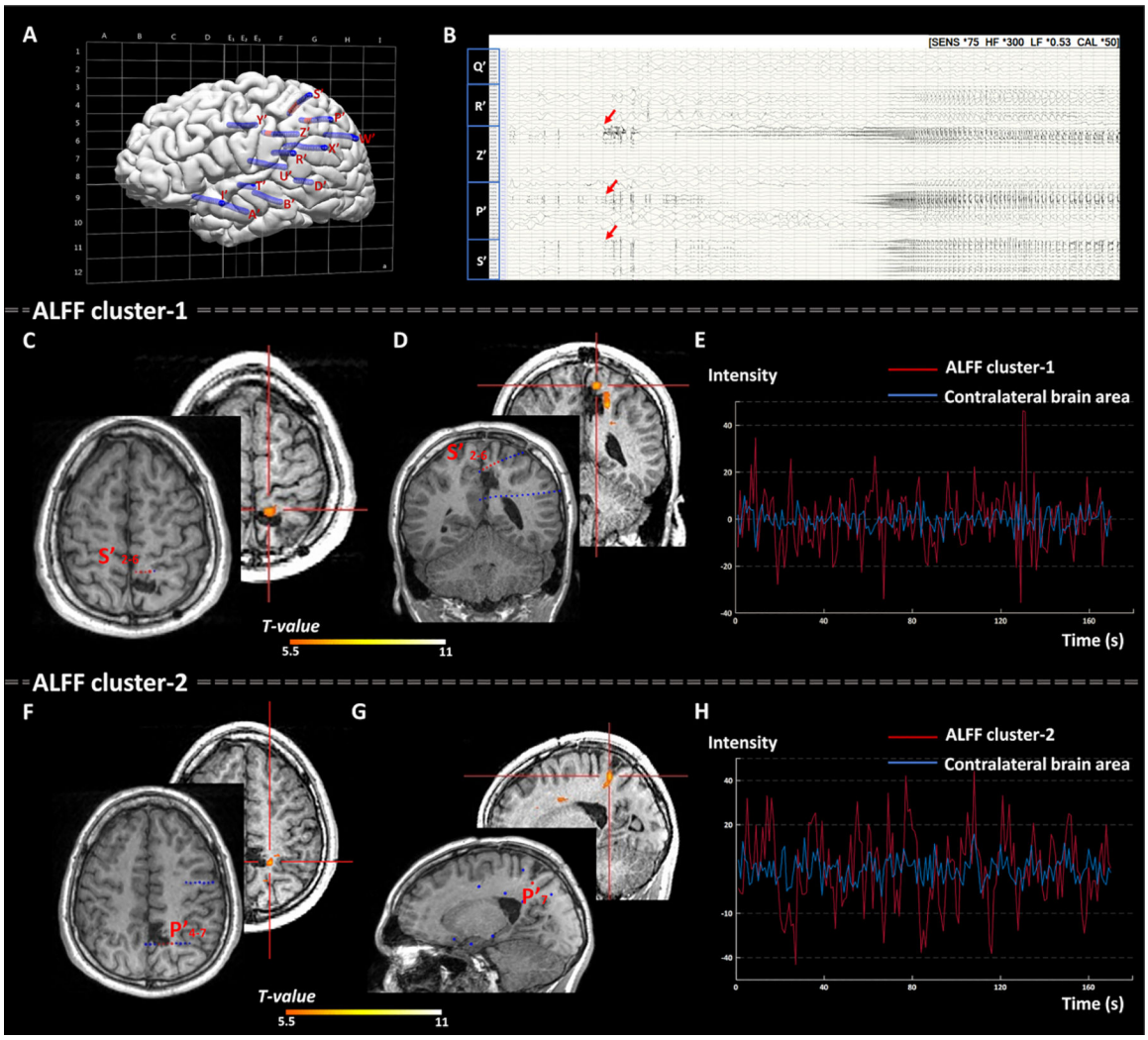

Figure 3:

Representative case 2: Illustration of two concordant ALFF clusters with the SOZ defined by SEEG in a patient with non-lesional MRI (P7 in table 1). SEEG was implanted based on the hypotheses including the posterior perisylvian, posterior insular/operculum, mesial parietal and cingulate areas in the left hemisphere. A) SEEG implantation map shown with Talairach grid superimposed, including 14 electrodes and 186 contacts (contacts indicating SOZ marked with red, other contacts marked with blue). B) Bipolar montage of relevant SEEG channels (50-second epoch): Typical seizure showed onset involving primarily contacts Z'3–5 (cingulate gyrus), P'4–7 and S'2–6 (dorsomedial parietal region) characterized by preictal spiking followed by EEG attenuation and paroxysmal fast discharge. C) Axial view and D) coronal view: ALFF cluster-1 with peak intensity, indicated by the red crossbar, concordant with the SOZ (noted by the red SEEG contacts S'2–6). F) Axial view and G) sagittal view: ALFF cluster-2 with 2nd peak intensity, indicated by the red crossbar, concordant with the SOZ (noted by the red SEEG contacts P'4–7). E) and H): time series graphs for ALFF cluster-1 and cluster-2 plotted separately to show the BOLD signal fluctuation versus time in seconds. Time series were extracted from the SOZ-concordant ALFF activation clusters in

the left supramarginal gyrus (red line) both showed significantly higher amplitude than that from the corresponding contralateral brain area (blue line), suggesting increase of regional neural activities within the SOZ. As shown in panels C, D, F and G, the 2 ALFF clusters and SEEG contacts were co-registered to the postoperative MRI. This patient didn't gain seizure-free due to the incomplete resection of the SEEG-defined SOZ as well as the ALFF clusters (because of nearby eloquent cortex).

ALFF= amplitude of low-frequency fluctuations; s= second; SOZ= seizure onset zone; SEEG= Stereo-electroencephalography; MRI= magnetic resonance imaging; BOLD= Blood oxygenation level dependent.

Table 1.

Clinical and demographic information of patients included in this study.

Pt No.	Sex	Age (yr)	Handedness	Age at Onset (yr)	Epilepsy Duration (yr)	Seizure Frequency	No. of ASMs	Brain MRI[a]	IEDs	SEEG-detected SOZ	Surgical Approach	Pathology[b]	Surgical Outcome[c]
1	F	23	R	17	6	Few times/ week	3	L TO CD	L FT/TP	L Basomesial T	L T Lobectomy	FCDI	ILAE-1
2	M	26	R	10	16	2–3/ week	5	NL	L T/FT	L Mesiobasal FT	NA	NA	NA
3	M	53	R	48	5	2–4/ week	4	NL	NA	L T Pole + Amy	L ATL sparing Hip	FCD IB	ILAE-1
4	M	56	R	5	51	Daily	3	Bi PNH	L TPO	L mesial T Nodule	Nodule ablation	NA	ILAE-1
5	F	56	R	36	20	Daily	3	NL	L TP/R T	L Mesial T	L ATL	FCD I	ILAE-5
6	M	45	R	37	8	1/ week	2	R PNH	NA	R PNH + Hip + Amy	Nodule ablation	NA	ILAE-1
7	M	17	R	2	15	Few times/ week	3	NL	L CP	L Mesial P	L mesial P corticectomy	FCD IIA	ILAE-4
8	M	39	R	11	28	Daily	1	NL	NA	L anterior In + ACC	NA	NA	NA
9	F	16	R	8	8	1–2/ month	2	Bi PNH	Bi TP	R PNH + Hip + Amy	R ATL	Heterotopia	follow-up < 1 yr
10	M	32	R	7	25	2–3/ week.	3	NL	NA	R superior T Gyrus	R lateral T corticectomy	FCD IC	ILAE-1
11	F	17	R	1	16	Daily	3	R In EM	NA	R orF	R orF corticectomy	FCD IIB	ILAE-1
12	M	18	R	6	12	1 cluster/ month	1	R PNH	R FP	R FT including PNH	Nodule ablation followed by R FT lobectomy	Heterotopia + FCD IB	follow-up < 1 yr
13	F	43	L	2	41	Daily	3	NL	Bi FT	L orF	L orF corticectomy	FCD IB	follow-up < 1 yr
14	F	18	R	9	9	Few times/ week	3	NL	NA	R In	R In ablation	NA	follow-up < 1 yr
15	M	25	R	20	5	Few times/ month	3	Bi PNH	R FT/L F	R PNH + lateral T + Pop	Nodule ablation	NA	follow-up < 1 yr
16	M	14	R	10	4	Daily	2	R P EM	R H/R CP	R mesial precuneus	R mesial P corticectomy	FCD IIA	follow-up < 1 yr
17	F	16	R	5	11	Daily	2	NL	R H	R lateral FP	NA	NA	NA
18	M	24	R	12	12	1/ 1–2 week	3	Bi PNH	Bi TPO	L Amy + R basal T including PNH	Nodule ablation	NA	follow-up < 1 yr

Pt No.	Sex	Age (yr)	Handedness	Age at Onset (yr)	Epilepsy Duration (yr)	Seizure Frequency	No. of ASMs	Brain MRI[a]	IEDs	SEEG-detected SOZ	Surgical Approach	Pathology[b]	Surgical Outcome[c]
19	M	21	L	16	5	Few times/ week	4	Bi PNH	NA	R PNH + Hip + Amy	R ATL	Heterotopia + FCD IB	follow-up < 1 yr

[a]MRI findings were defined by official radiological report.

[b]Pathology were classified based on the ILAE 2016 recommendation of neuropathologic workup of epilepsy surgery brain tissue and the ILAE 2011 FCD classification guidelines.

[c]Surgical outcome was defined by the ILAE classifications in patients with > 1 year postoperative follow-up.

Pt No.= patient number; yr= years; No. of ASMs = number of antiseizure medications; MRI= magnetic resonance image; IEDs = interictal epileptiform discharges on scalp EEG; SEEG= Stereo-electroencephalography; SOZ= seizure onset zone; F= female; M= male; R= right; L= left; TO= temporooccipital; CD= cortical dysplasia; FT= frontotemporal; TP= temporoparietal; T= temporal; FCD= Focal cortical dysplasia; ILAE= international league against epilepsy; NL= non-lesional; NA= not available; Amy= amygdala; ATL= anterior temporal lobectomy; Hip= hippocampus; TPO= temporo-parieto-occipital; Bi= bilateral; PNH= periventricular nodular heterotopia; CP= centroparietal; P= parietal; In= insula; ACC= anterior cingulate cortex; EM= encephalomalacia; orF= orbital frontal; FP= frontoparietal; F= frontal; Pop = parietal operculum; H= hemisphere.

Table 2.

Performance of rsfMRI metrics on co-localization of SEEG-defined SOZ.

	Concordant pt no.	Concordant rate	95% CI	Sensitivity	95% CI	PPV	95% CI
ALFF	Concordance: n=14 Discordance: n=4 Negative: n=1	73.7% (14/19)	48.8% – 90.9%	93.3%	66.0% – 99.7%	77.8%	51.9% – 92.6%
ReHo	Concordance: n=2 Discordance: n=6 Negative: n=11	10.5% (2/19)	1.3% – 33.1%	15.4%	2.7% – 46.3%	25.0%	4.5% – 64.4%
DC	Concordance: n=3 Discordance: n=4 Negative: n=12	15.8% (3/19)	3.4% – 39.6%	20.0%	5.3% – 48.6%	42.9%	11.8% – 79.8%

RsfMRI= resting-state functional magnetic resonance image; SEEG= stereo-electroencephalography; SOZ= seizure onset zone; pt no.= patient number; CI= confidence interval; PPV= positive predictive value; ALFF= amplitude of low frequency fluctuations; ReHo= regional homogeneity; DC= degree centrality.

Table 3.

Concordance between ALFF clusters and SEEG-defined SOZ sub-classified by clinical characteristics.

	ALFF			χ^2	p value[a]
	Concordant no. (%)	Discordant no. (%)	Negative no. (%)		
Brain MRI [b]				1.29	0.78
Non-lesional (n=9)	6 (66.7)	2 (22.2)	1 (11.1)		
Lesional (n=10)	8 (80.0)	2 (20.0)	None		
Interictal scalp EEG				2.41	0.36
With IEDs (n=12)	10 (83.3)	2 (16.7)	None		
Without IEDs (n=7)	4 (57.1)	2 (28.6)	1 (14.3)		
Epileptic syndrome				1.83	0.58
TLE (n=9)	7 (77.8)	1 (11.1)	1 (11.1)		
ETLE (n=10)	7 (70.0)	3 (30.0)	None		
SOZ distribution				4.98	0.07
Deep-seated area (n=16)	13 (81.3)	3 (18.7)	None		
Convexity of brain (n=3)	1 (33.3)	1 (33.3)	1 (33.3)		
Pathology (n=11) [c]				8.99	0.36
FCD I (n=7 [d])	6 (85.7)	None	1 (14.3)		
FCD IIA (n=2)	2 (100.0)	None	None		
FCD IIB (n=1)	None	1(100.0)	None		
Heterotopia (n=1)	1(100.0)	None	None		
Surgical outcome [e] (n=8)				1.21	1.00
Seizure-free (n=6)	4 (66.7)	1 (16.7)	1 (16.7)		
Non-seizure-free (n=2)	2 (100.0)	None	None		

[a] Statistical threshold was set at P< 0.05, two tailed.

[b] MRI findings were defined by official radiological report.

[c] FCD lesions were classified based on the ILAE 2016 recommendation of neuropathologic workup of epilepsy surgery brain tissue and the ILAE 2011 FCD classification guidelines.

[d] Two patients with double pathology (P12 and P19 in Table 1), whose concordant ALFF clusters were located in the dysplastic tissue, were included under the FCD category.

[e] Surgical outcome was defined by the ILAE classification and dichotomized as seizure-free (only including ILEA-1) or non-seizure-fee in patients with > 1 year postoperative follow-up.

ALFF= amplitude of low frequency fluctuations; SEEG= Stereoelectroencephalography; SOZ= seizure onset zone; no.= number; MRI= magnetic resonance image; EEG= electroencephalography; IEDs = interictal epileptiform discharges; TLE= temporal lobe epilepsy; ETLE= extratemporal lobe epilepsy; FCD= Focal cortical dysplasia